J. Mol. Biol. (1997) **270**, 763–770

JMB

A Comparison of the Folding Kinetics and Thermodynamics of Two Homologous Fibronectin Type III Modules

Kevin W. Plaxco, Claus Spitzfaden, Iain D. Campbell and Christopher M. Dobson*

Oxford Centre for Molecular Sciences, New Chemistry Laboratory and The Department of Biochemistry, University of Oxford, South Parks Road Oxford OX1 3QT, England

**Corresponding author*

The homologous ninth and tenth type III modules of human fibronectin share identical topologies and nearly identical core structures. Despite these structural similarities, the refolding characteristics of the two modules, which have a sequence identity of less than 30 %, are very different; in the absence of denaturant the ninth module folds several hundred times more slowly than the tenth and, although both modules contain numerous proline residues, only the ninth exhibits a slow, proline isomerization-limited folding phase. The different folding kinetics of the two modules coincide with a large difference in their thermodynamic stability, with the folding free energy of the tenth being approximately five fold greater than that of the ninth. This may be the reason why the ninth module, unlike the rapidly folding tenth module, is apparently unable to overcome characteristics of the fibronectin type III modules that can slow the folding process. The non-proline-limited folding kinetics are, however, very similar for the two modules when compared under conditions where their overall stabilities are similar. The significance of this finding is discussed in terms of possible determinants of the kinetics of protein folding.

Keywords: Fibronectin type III; proline isomerization; protein folding; stability

Introduction

The spontaneous refolding of proteins occurs with time constants ranging from milliseconds to hours (e.g. see Jackson & Fersht, 1991; Huang & Oas, 1995; Kragelund *et al.*, 1995; Kern *et al.*, 1995). While primary sequence is presumably the ultimate determinant of these rates, many factors such as protein size, topology, proline content and thermodynamic stability are thought to play a role in this large range of kinetic behaviour (Creighton, 1978; Kiefhaber *et al.*, 1992; Orengo *et al.*, 1994; Bryngelson *et al.*, 1995; Fersht, 1995; Onuchic *et al.*, 1995; Gross, 1996; Mines *et al.*, 1996; Miranker & Dobson, 1996). Discriminating between the contributions of each of these properties to the kinetics of protein folding would require the ability to vary each characteristic independently. While this has not yet proved feasible, the study of the refolding kinetics of members of homologous protein families should provide a means of examining the role that sequence and stability play in determining folding kinetics in the absence of complicating factors such as significantly different topologies or structures.

One of the largest known families of homologous proteins is that of the fibronectin type III modules (FNIII), of which more than 400 examples are known (Bork *et al.*, 1996). In order to investigate the relationship between the folding character-

Present addresses: K. W. Plaxco, Department of Biochemistry, Box 357350, University of Washington, Seattle, WA 98195, USA; C. Spitzfaden, SmithKline Beecham Pharmaceuticals, Computational and Structural Sciences, Harlow, CM19 5AW, England.

Abbreviations used: FNIII, fibronectin type III; ^{9}FNIII and ^{10}FNIII, the ninth and tenth FNIII modules of human fibronectin, respectively; TnfN3, the third FNIIII domain of human tenascin; ΔG_f, the free energy of unfolding; GuHCl, guanidine hydrochloride; m_{eq}, the dependence of the free energy of unfolding on [GuHCl]; $m_f^{\ddagger}$, the dependence of the folding activation energy on [GuHCl]; θ_m, the ratio $m_f^{\ddagger}/ m_{eq}$; PPI, peptidyl prolyl isomerase; rmsd, root-mean-square deviation.

0022–2836/97/300763–08 $25.00/0/mb971148

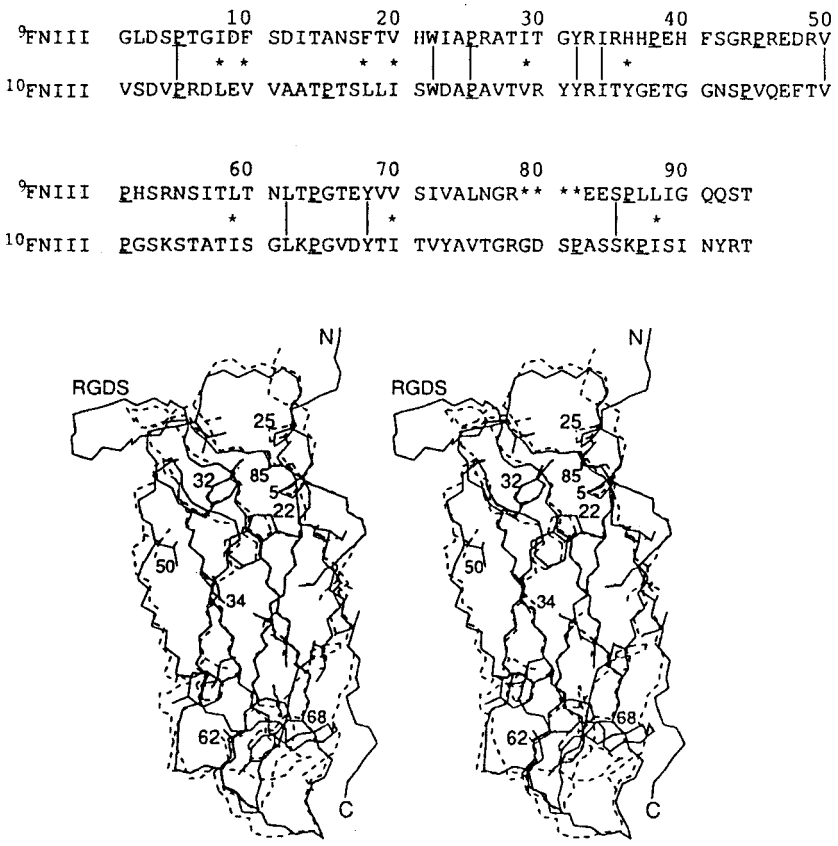

Figure 1. A comparison of the sequences and structures of ^{9}FNIII and ^{10}FNIII. Upper, A sequence alignment of ^{9}FNIII and ^{10}FNIII. Sequence identity is only moderate (28%) but overall sequence similarity is high and key elements of the hydrophobic core are either identical (vertical bars) or conservatively replaced (*). Proline residues are underscored to illustrate the relatively high proline content of the two modules and the degree of conservation of these residues. The four-residue insertion in ^{10}FNIII (containing the integrin-binding RGD sequence) is known to be disordered in solution (Main *et al.*, 1992; Dickinson *et al.*, 1994). Lower, An overlay of the backbone conformations of ^{9}FNIII and ^{10}FNIII (Leahy *et al.*, 1996). Core residue main chain atoms exhibit an rmsd of 0.72 Å. The side-chains of identical core residues are indicated. These share, to within experimental error, identical conformations in the two structures.

istics of distantly homologous proteins, we have investigated the folding thermodynamics and kinetics of two members of this family, the ninth and tenth FNIII modules of human fibronectin (^{9}FNIII and ^{10}FNIII). These modules comprise seven β-strands arrayed in two topologically complex sheets (Figure 1: Main *et al.*, 1992). The ^{10}FNIII module contains eight proline residues, with at least one in each of the seven intra-strand loops. Previous research indicates that despite its proline-rich all β-sheet structure the ^{10}FNIII module refolds very rapidly; in 0.64 M guanidine hydrochloride (GuHCl) the domain appears to recover fully native core and backbone structures within one second at 5°C (Plaxco *et al.*, 1996). The ^{9}FNIII module is slightly smaller (90 residues instead of 94) and contains only seven proline residues. We report here a detailed thermodynamic and kinetic analysis of the folding of both the ^{10}FNIII and ^{9}FNIII domains. The folding kinetics and thermodynamics of a related FNIII module, the third FNIII module of tenascin (TnfN3) are described by Clarke *et al.* (1997) in the accompanying paper.

Results

Equilibrium stability

Equilibrium chemical denaturation studies indicate that the ^{10}FNIII module is significantly more stable than its homologue (Figure 2). With an equilibrium stability (ΔG_f) of $-6.1(\pm0.1)$ kcal mol^{-1}, the ^{10}FNIII module is relatively stable for such a small, non-disulphide-bonded protein. Conversely, equilibrium denaturation studies suggest the ^{9}FNIII module is relatively unstable, with a ΔG_f of only $-1.2(\pm0.5)$ kcal mol^{-1}. Unfortunately, due to the relatively low stability of the module, it has not proven possible to measure a significant pre-transition baseline, which accounts for the rather poor precision of the stability measurement. Nevertheless, the estimated stability is in good agreement with the results of previous, limited studies of the urea denaturation and the folding and unfolding rates of the module, which indicate ΔG_f to be approximately -1 kcal mol^{-1} (Spitzfaden *et al.*, 1997; and our, unpublished results). The dependence of the free energy of unfolding on GuHCl concentration ($m_{eq} = d\Delta G_f/d[GuHCl]$) also differs significantly between the two modules. The folding free energy of ^{10}FNIII is relatively unaffected by the presence of denaturant ($m_{eq} = 1.42(\pm0.02)$ kcal mol^{-1} M^{-1}). The ^{9}FNIII module is significantly more sensitive to the presence of the denaturant ($m_{eq} = 3(\pm 1)$ kcal mol^{-1} M^{-1}). This difference is perhaps surprising, as m_{eq} is thought to reflect the relative solvent-accessible surface area of the unfolded state and thus it tends to be similar for proteins of similar structure (Myers *et al.*, 1995). Indeed, the value obtained for ^{9}FNIII is close to those observed for other small, single domain proteins (see Myers *et al.* (1995) and the accompanying

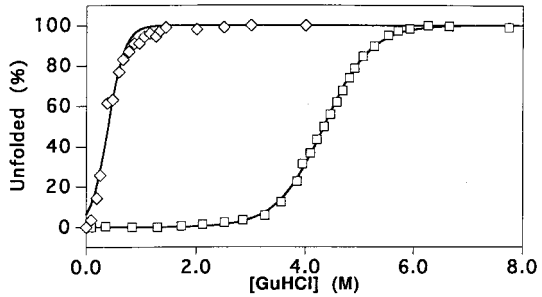

Figure 2. Equilibrium denaturation curves for the GuHCl unfolding of ^{9}FNIII (diamonds) and ^{10}FNIII (squares). Both proteins denature in a cooperative fashion with free energies of unfolding of $-1.2(\pm0.5)$ kcal mol^{-1} and $-6.1(\pm0.1)$ kcal mol^{-1} and m_{eq} values of ~3 kcal mol^{-1} M^{-1} and 1.4 kcal mol^{-1} M^{-1}, respectively.

paper by Clarke *et al.* (1997) and note that *m*(GuHCl) is often approximately twice *m*(urea) (Myers *et al.*, 1995)). While the origin of these differences remains unclear, it is evident that ^{9}FNIII is significantly less stable than ^{10}FNIII despite the nearly identical core structure of the two modules.

Refolding kinetics of ^{9}FNIII

The refolding of the ^{9}FNIII domain is relatively slow. The kinetics of the recovery of native tryptophan fluorescence during the refolding of ^{9}FNIII are illustrated in Figure 3A. The data are fit well by a sum of two exponentials (residual amplitudes <2%), suggesting that two significant processes are occurring during refolding. The refolding kinetics are effectively identical whether monitored by flu-

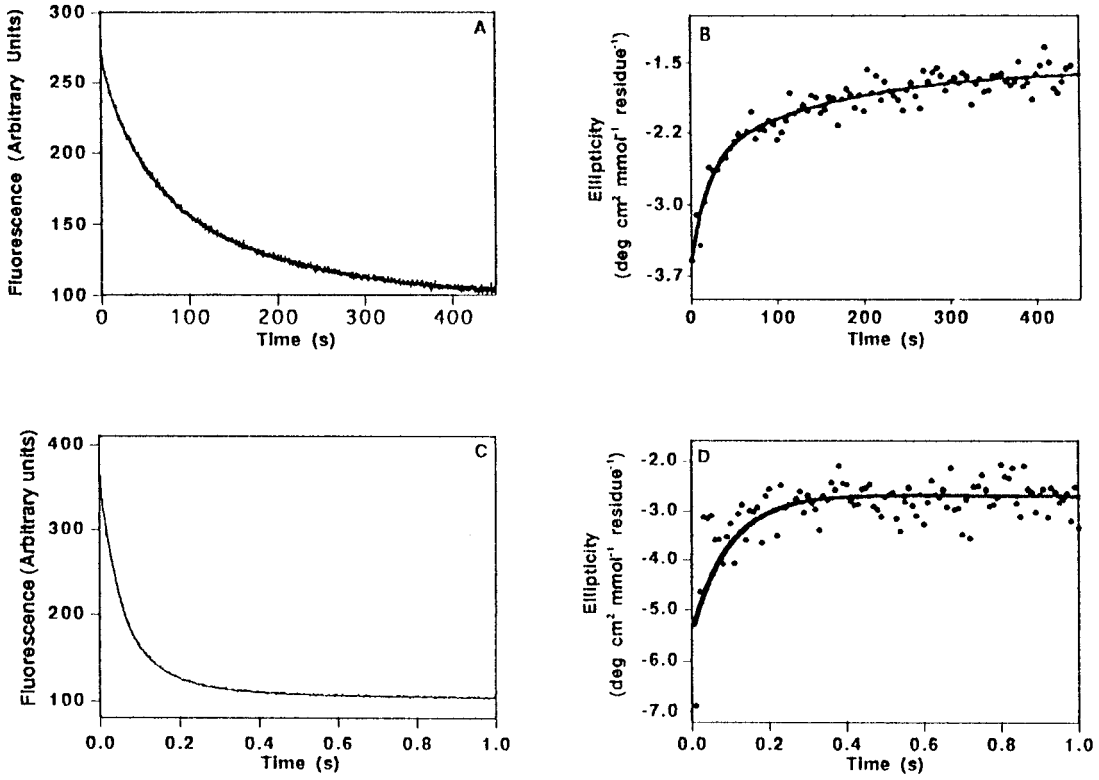

Figure 3. The kinetics of the recovery of fluorescence (A and C) and far-UV CD (B and D) during refolding of ^{9}FNIII and ^{10}FNIII at 5°C. The large difference in the refolding rates of these proteins is readily apparent in the differing ordinate scales. The kinetics of the recovery of native tryptophan fluorescence is thought to correlate with the recovery of native core packing. For ^{9}FNIII (A) the data fit well to the sum of two exponential processes with rate constants of 0.032(±0.001) and 0.0075(±0.0002) s^{-1} and relative amplitudes of 38(±2)% and 62(±2)%, respectively. The recovery of native far-UV CD signal at 216 nm (B) reflects the recovery of a native backbone conformation. These data are fit as the sum of two exponential processes with rate constants of 0.049(±0.022) and 0.006(±0.002) s^{-1} and relative amplitudes of 51(±19)% and 49(±14)%, respectively. These data suggest that the refolding of ^{9}FNIII is a cooperative event lacking significantly populated intermediates with non-native CD or fluorescence properties. The refolding of the ^{10}FNIII module, while orders of magnitude faster, is also cooperative. The recovery of native fluorescence (C) occurs with rate constants of 19.6(±0.1) and 5.43(±0.03) s^{-1} and relative amplitudes of 77(±3) and 23(±3)%, and the recovery of native far-UV CD (D) is characterized by a rate of 18.2(±2.1) s^{-1}. The poor signal-to-noise ratio of far-UV CD signals precludes the observation of the smaller amplitude phase. These experiments were conducted at pH 5.2 with final GuHCl concentrations of 0.182 M (^{9}FNIII) and 0.636 M (^{10}FNIII). C and D are adapted from Plaxco *et al.* (1996).

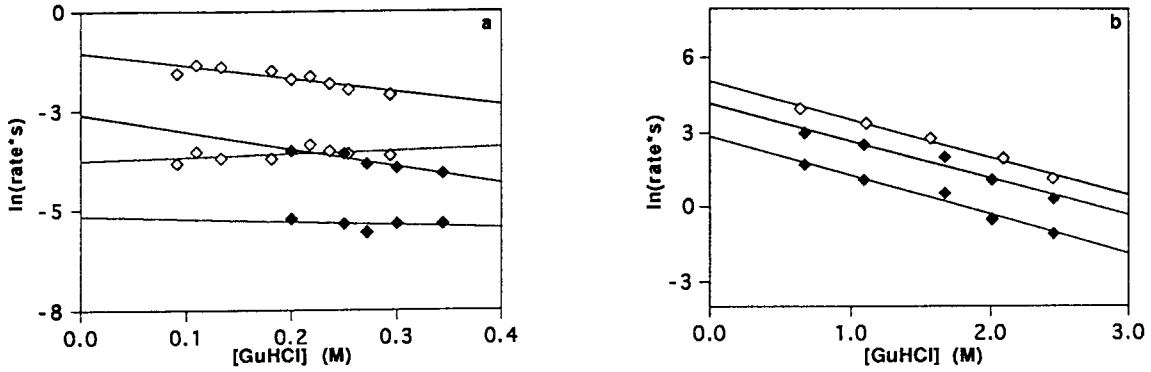

Figure 4. The refolding kinetics of ^{9}FNIII (a) and ^{10}FNIII (b) as a function of final GuHCl concentration at 5°C (filled symbols) and 25°C (open symbols). Only a single refolding phase is observed for ^{10}FNIII at the higher temperature.

orescence or far ultraviolet circular dichroism (far UV-CD) (Figure 3B). The effects of GuHCl on the rates of these two folding reactions are presented in Figure 4a, from which the intrinsic rates (the rates at 0 M GuHCl) and GuHCl sensitivities ($m_f^{\ddagger} = d\Delta G^{\ddagger}/d[GuHCl]$) of the two processes can be estimated. Linear extrapolation of a plot of ln(k) *versus* GuHCl concentration to 0 M GuHCl indicates that the intrinsic rate constants of these processes are 0.4(±0.2) and 0.024(±0.002) s^{-1} at 25°C (Figure 4a). These data also suggest that while the rate constant of the faster reaction is significantly reduced by the presence of GuHCl ($m_f^{\ddagger}$ at 25°C = 1.9(±0.5) kcal mol^{-1} M^{-1}), the slower reaction remains effectively unchanged by increasing amounts of the denaturant ($m_f^{\ddagger} = -0.5(\pm0.7)$ kcal mol^{-1} M^{-1}). At 5°C the refolding of ^{9}FNIII remains biphasic with intrinsic rate constants of $7(\pm1) \times 10^{-2}$ and $6(\pm1) \times 10^{-3}$ s^{-1} (Figure 4a). The relative amplitudes of these two phases are unaffected by increases in GuHCl concentration and remain at 33(±3)% and 67(±3)% for the fast and slow reactions, respectively. The relatively large standard errors of the measurements of the intrinsic refolding rates and $m_f^{\ddagger}$ of this module reflect the small range of GuHCl concentrations over which the module is stable. The ratio $m_f^{\ddagger}/m_{eq}$, θ_m, is 0.7, which suggests that the transition state of the folding of ^{9}FNIII is relatively compact (Chen *et al.*, 1992).

Refolding kinetics of ^{10}FNIII

The refolding of ^{10}FNIII is relatively fast. The refolding kinetics are biphasic at low temperatures (Plaxco *et al.*, 1996) with intrinsic rate constants of 64(±2) and 17(±2) s^{-1} at 5°C (Figure 4b). The relative amplitudes of these phases are unaffected by GuHCl and remain at 70(±3)% and 30(±3)%, respectively. At higher temperatures the rates and amplitudes of the two phases become similar and at 25°C only a single folding phase can be distinguished. The intrinsic refolding rate constant of ^{10}FNIII under these conditions is 155(±5) s^{-1} (Figure 4b). The folding transition state energetics of ^{10}FNIII at 25°C are relatively insensitive to the presence of denaturant ($m_f^{\ddagger} = 0.91(\pm0.03)$ kcal mol^{-1} M^{-1}). The two refolding phases observed at lower temperatures exhibit effectively identical GuHCl sensitivities (fast, $m_f^{\ddagger} = 0.84(\pm0.02)$ kcal mol^{-1} M^{-1}; slow, $m_f^{\ddagger} = 0.86(\pm0.02)$ kcal mol^{-1} M^{-1}), suggesting that the changes in solvent-exposed surface area upon formation of the transition states of the two processes are very similar (Pace, 1986; Chen *et al.*, 1992). For ^{10}FNIII, θ_m is also 0.7, which suggests that its folding transition state may exhibit a similar degree of collapse.

The kinetic effects of pH and proline isomerization

In order to investigate possible reasons for the slow folding of ^{9}FNIII we have studied the effects of pH and peptidyl prolyl isomerase (PPI) on its refolding kinetics. The relatively large histidine content of ^{9}FNIII (while ^{10}FNIII lacks histidine ^{9}FNIII contains five histidine residues) could play a role in the slow folding of this module. Studies of the refolding of ^{9}FNIII as a function of pH, however, indicate that while the refolding rate of this protein is pH-dependent, the fast refolding rate exhibits only a 3.8-fold increase over the pH range 5.2 to 8.2. Further experiments aimed at elucidating the reasons for the relatively slow folding of ^{9}FNIII focused on the observation that, as is the case for proline isomerization (Creighton, 1978), the rate and relative amplitude of the slow folding phase of ^{9}FNIII are not affected by changes in GuHCl concentration. That proline isomerisation limits the rate is further supported by studies of the effect of PPI on the refolding rates of ^{9}FNIII; the addition of 4 μM PPI speeds the rate of the slowest phases of the refolding of ^{9}FNIII by a factor of 3 (0.02 to 0.06 s^{-1} at 25°C, pH 5.2). That the slow process in ^{10}FNIII folding is both orders of magnitude faster than previously characterized proline isomerization events (Creighton, 1978) and relatively sensi-

tive to GuHCl suggests that it is not a simple, proline isomerization-limited process.

Discussion

Previously reported studies suggest that structural differences between these two homologous domains are small despite a relatively low level of sequence identity (Leahy *et al.*, 1996). Sequence alignment of ^{9}FNIII and ^{10}FNIII indicates that the two modules share 28% sequence identity (Figure 1: Kornblihtt *et al.*, 1985). Sequence and structural alignments both show that ^{10}FNIII contains a four-residue insertion lacking in ^{9}FNIII. This element, comprised of residues 78 to 81 of ^{10}FNIII, corresponds to the RGD-cell adhesion site of fibronectin and is not present in ^{9}FNIII or well ordered in ^{10}FNIII (Main *et al.*, 1992; Dickinson *et al.*, 1994). Structurally, these FNIII modules are otherwise very similar; their structures superimpose with a backbone rmsd of only 0.72 Å for the regular elements of secondary structure, well within the limits of resolution of the crystal structure (Figure 1: Leahy *et al.*, 1996). Within the regular secondary structure, notable rmsd and ϕ and φ backbone angle deviations are limited to the β-bulge of residues 11 and 12. The packing of conserved side-chains in the hydrophobic cores of the modules also exhibits a very high degree of similarity, with the structures of all conserved residues in the two modules identical to within the resolution of the crystal structure (Figure 1). The loop regions of the two modules are less similar, the largest deviations between the two structures occurring in the loop between β-strands C and C′. If loop residues are included in the superposition, the backbone rmsd increases to 1.68 Å (unpublished results). This full superposition rmsd is, however, presumably an overestimate of the structural divergence of the two modules as NMR studies (Main *et al.*, 1992; our unpublished results) indicate that many of the loops are relatively flexible in solution; comparison of the static crystal structure coordinates may therefore overestimate the structural divergence of these regions.

The limited evidence available suggests that both modules fold *via* qualitatively similar, two-state kinetics and that the relatively slow folding of ^{9}FNIII is not due to complications such as the formation of a non-productive intermediate (e.g. Sosnick *et al.*, 1993) or the occurrence of a significant, slowly folding on-pathway intermediate (e.g. Dobson *et al.*, 1994). Unlike the recovery of native fluorescence, which provides a probe of the formation of native core contacts, the recovery of far-UV CD ellipticity monitors the rate of formation of native secondary structure (Plaxco & Dobson, 1996). The kinetics of the recovery of the native ^{9}FNIII CD signal and fluorescence are effectively identical, suggesting that the folding of this protein is cooperative and does not progress *via* significantly populated kinetic intermediates with non-native fluorescence or backbone conformation (Figure 3). Further evidence that the biphasic folding kinetics of ^{9}FNIII represent two cooperative parallel folding pathways is that the relative amplitudes of the two processes remain unchanged over the range of GuHCl concentrations monitored. As both sequential and trapped pathways are predicted to show a strong dependence of relative amplitudes on the rates of the reactions involved (Ikai & Tanford, 1971), these data are consistent with the observed biphasic folding kinetics reflecting the heterogeneity of the denatured state rather than the occurrence of folding intermediates. The amplitudes of the two low-temperature refolding phases of ^{10}FNIII also remain unchanged over a wide range of GuHCl concentrations. This is consistent with the previously reported (Plaxco *et al.*, 1996) observation that, like ^{9}FNIII, the TnFN3 domain (see the accompanying paper, Clarke *et al.*, 1997) and numerous other small, single domain proteins (e.g. see Jackson & Fersht, 1991; Schindler *et al.*, 1995; Kragelund *et al.*, 1996) ^{10}FNIII folds in a cooperative process (Figure 3C and D) lacking significant kinetic intermediates.

Despite this simple, qualitative similarity the intrinsic refolding rates of ^{9}FNIII and ^{10}FNIII differ by up to three orders of magnitude. This is in contrast with previously described sets of homologous proteins, which tend to share qualitatively similar folding pathways and relatively similar refolding rates. The study of several avian and mammalian lysozymes, with sequence identities ranging from 61 to 95%, has indicated that these proteins exhibit broadly similar refolding behaviour that differs primarily in the population of a single, well-defined intermediate state and exhibit only a fourfold range of refolding rates (Hooke *et al.*, 1994, 1995; D. Haynie & N. Woodruff, personal communication). The characterization of bovine, rat and yeast acyl-coenzyme A carrier binding protein (43 to 84% sequence identity) suggests that despite a 15-fold range of intrinsic refolding rates these three proteins fold with qualitatively similar two-state kinetics (Kragelund *et al.*, 1996). The dependence of the relative refolding rates of yeast and horse heart cytochrome *c* on GuHCl, proteins exhibiting 60% sequence identity and a 25-fold difference in intrinsic refolding rates, suggests that the folding transition regions of these proteins are similarly placed on their respective folding pathways and that the two proteins fold in a qualitatively similar fashion (Nall & Landers, 1981; Mines *et al.*, 1996; J. Winkler, personal communication). Thus it is perhaps surprising that a pair of homologous FNIII modules can span two to three of the six orders of magnitude range of previously characterized protein folding rates.

With seven trans proline residues in ^{9}FNIII and eight in ^{10}FNIII, at least 50 to 60% of denatured protein molecules should contain one or more incorrectly configured proline residues (Creighton, 1978). This may be reflected in the 67% amplitude

slow phase evident in the refolding of ^{9}FNIII with a rate, GuHCl and PPI dependence characteristic of proline isomerization. Despite a higher proline content, which, if anything, might suggest it would be the slower folding of the two modules, the ^{10}FNIII module lacks a detectable proline isomerization-like folding phase. This has been postulated to be due to either folding-induced acceleration of the isomerization rate in a stable, native-like intermediate or to the fact that the protein folds to a stable and extremely native-like conformation as yet indistinguishable from the native protein (Cook *et al.*, 1979; Schmid & Blaschek, 1981; Evans *et al.*, 1989; Plaxco *et al.*, 1996). Presumably neither of these mechanisms would be accessible to the much less stable ^{9}FNIII module.

While 33% of denatured ^{9}FNIII molecules fold in a reaction that is not limited by proline isomerization, they still fold at a rate hundreds of times slower than the refolding rates of ^{10}FNIII. This difference might also be attributable to the relative stability of the two modules. Under conditions in which the stability of ^{10}FNIII is similar to the intrinsic stability of ^{9}FNIII (about -1.2 kcal mol^{-1}) its refolding rate constant is $0.8(\pm0.1)$ s^{-1} (at 3.45 M GuHCl; from Figure 2 and 4). This is very similar to the $0.4(\pm0.2)$ s^{-1} intrinsic refolding rate constant of ^{9}FNIII. The observed coincidence of rates would occur if two relationships are true: (1) θ_m is the same for both proteins; and (2) the ratio of the difference in the intrinsic folding activation energies of the two homologues, $\Delta\Delta G_f^{\ddagger}$, to the difference in their equilibrium stabilities, $\Delta\Delta G_f$, is approximately equal to θ_m . That these proteins exhibit equivalent θ_m values is verified by experiment and presumably reflects the fact that, like the native structures, the structures of the folding transition states of these two distantly homologous modules are very similar. The origins of the second relationship are less clear, but it may indicate that θ_m is a good approximation of the fraction of native, thermodynamically important contacts formed in the transition state. These results are consistent with recent experimental (Mines *et al.*, 1996) and theoretical (Finkelstein, 1991; Sali *et al.*, 1994; Bryngelson *et al.*, 1995; Onuchic *et al.*, 1995) evidence that the protein folding kinetics of at least some homologous proteins parallel closely native state stabilities and suggest that the 400 to 900-fold difference in the non-proline-limited refolding rates of these distantly homologous proteins may, because of the conserved nature of their folding transition states, be almost entirely attributed to differences in their equilibrium stabilities.

Methods

Protein purification and equilibrium denaturation

Recombinant human ^{9}FNIII and ^{10}FNIII were expressed as individual proteins in the form of glutathione-*S*-transferase fusions in *Escherichia. coli* and purified as described (Mardon & Grant, 1994). Equilibrium unfolding experiments were conducted on samples incubated with various concentrations of GuHCl in 20 mM sodium acetate (pH 5.2) for ten minutes with a Perkin Elmer LS 50B fluorimeter held at to $25(\pm1)^{\circ}$C. Excitation was at 280 nm, and emission was monitored at $350(\pm10)$ nm. Final GuHCl concentrations were determined by refractometry (Nozaki, 1972). Thermodynamic parameters were calculated with the non-linear least-squares fitting algorithm in KaleidaGraph (Abelbeck Software, Reading, PA) as described (Spitzfaden *et al.*, 1997).

Refolding kinetics

Refolding kinetics were monitored by following the recovery of native fluorescence and far-UV CD. Kinetic fluorescence data for the refolding of ^{10}FNIII were obtained with a SX17-MV stopped-flow fluorimeter, held at $5(\pm0.1)$ or $25(\pm0.1)^{\circ}$C, as described (Plaxco *et al.*, 1996). Kinetic fluorescence data for the refolding of ^{9}FNIII were obtained using either the SX17-MV or a Perkin Elmer LS 50B fluorimeter controlled to within ±0.5 deg. C and coupled to a pneumatic mixer as described (Balbach *et al.*, 1995). Kinetic fluorescence data were collected for ^{9}FNIII or ^{10}FNIII (0.1 to 0.2 mM) in 2.0 M or 7.0 M GuHCl, respectively, diluted 11-fold with acetate (20 mM sodium acetate, pH 5.2), 20 mM sodium phosphate (pH 6.2), 20 mM Tris-HCl (pH 7.2 or 8.2), or the appropriate GuHCl concentration in acetate. Additionally, some ^{9}FNIII samples were diluted 21-fold with GuHCl/acetate solutions. PPI (cyclophilin A: a generous gift from Dr S. E. Jackson; Department of Chemistry, Cambridge, England), at approximately 2 to 4 μM, was included in the refolding buffer as appropriate. Far-UV CD results were obtained using a J720 spectropolarimeter (Jasco, Tokyo, Japan) coupled to a SFM3 stopped-flow module (Biologic, Claix, France) held at $5.0(\pm0.5)^{\circ}$C, as described (Plaxco *et al.*, 1996). ^{9}FNIII (0.2 mM) in 2.0 M GuHCl was diluted 11-fold with acetate and the ellipticity at $216(\pm2)$ nm was followed. The data were fit to exponential decay curves using the non-linear least-squares fitting software supplied with the Applied Photophysics fluorimeter or with KaleidaGraph. Reported values reflect either the average and standard deviation of five to ten experiments (fluorescence kinetics) or estimated fitting errors.

Acknowledgements

We thank Jane Clarke for many valuable discussions and for sharing unpublished data, Helen Mardon and Kate Grant for providing the FNIII-GST fusion clones, Sophie Jackson for providing PPI, Cameron Marshall for aid in conducting equilibrium unfolding experiments, Craig Morton for providing artistic advice, and Jay Winkler, Don Haynie and Nick Woodruff for communicating unpublished results. The Oxford Centre for Molecular Sciences is supported by the U.K. Biotechnology and Biological Sciences Research Council, the Engineering and Physical Sciences Research Council, and the Medical Research Council. This work was also supported in part by a grant from the Wellcome Trust (to I.D.C.) and an International Research Scholars award from the Howard Hughes Medical Institute (to C.M.D.).

References

Balbach, J., Forge, V., van Nuland, N. A., Winder, S. L., Hore, P. J. & Dobson, C. M. (1995). Following protein-folding in real-time using NMR-spectroscopy. *Nature Struct. Biol.* **2**, 866–870.

Bork, P., Downing, A. K., Kieffer, B. & Campbell, I. D. (1996). Structure and distribution of modules in extracellular proteins. *Quart. Rev. Biophys.* **29**, 119–167.

Bryngelson, J. D., Onuchic, J. N., Socci, N. D. & Wolynes, P. G. (1995). Funnels, pathways, and the energy landscape of protein-folding–a synthesis. *Proteins: Struct. Funct. Genet.* **21**, 167–195.

Clarke, J., Hamill, S. J. & Johnson, C. M. (1997). Folding and stability of a fibronectin type III domain of human tenacin. *J. Mol. Biol.* **270**, 771–778.

Cook, K. H., Schmid, F. X. & Baldwin, R. A. (1979). Role of proline isomerization in folding of ribonuclease A at low temperature. *Proc. Natl Acad. Sci. USA,* **76**, 6157–6161.

Chen, B.-L., Baase, W. A., Nicholson, H. & Schellman, J. A. (1992). Folding kinetics of T4 lysozyme and nine mutants at 12°C. *Biochemistry,* **31**, 1464–1476.

Creighton, T. E. (1978). Possible implications of many proline residues for the kinetics of protein unfolding and refolding. *J. Mol. Biol.* **125**, 401–406.

Dickinson, C. D., Veerapandian, B., Dai, X. P., Hamlin, R. C., Xuong, N. H., Ruoslahti, E. & Ely, K. R. (1994). Crystal-structure of the 10th type-III cell-adhesion module of human fibronectin. *J. Mol. Biol.* **236**, 1079–1092.

Dobson, C. M., Evans, P. A. & Radford, S. E. (1994). Understanding how proteins fold–the lysozyme story so far. *Trends. Biol. Sci.* **19**, 31–37.

Evans, P. A., Kautz, R. A., Fox, R. O. & Dobson, C. M. (1989). A magnetic-transfer nuclear magnetic resonance study of the folding of staphylococcal nuclease. *Biochemistry,* **28**, 362–370.

Fersht, A. R. (1995). Optimization of rates of protein folding - the nucleation condensation mechanism and its implications. *Proc. Natl Acad. Sci. USA,* **92**, 10869–10873.

Finkelstein, A. V. (1991). Rate of β-structure formation in polypeptides. *Proteins: Struct. Funct. Genet.* **9**, 23–27.

Gross, M. (1996). Linguistic analysis of protein folding. *FEBS Letters,* **390**, 249–252.

Hooke, S. D., Radford, S. E. & Dobson, C. M. (1994). The refolding of human lysozyme: a comparison with the structurally homologous hen lysozyme. *Biochemistry,* **33**, 5867–5876.

Hooke, S. D., Eyles, S. J., Miranker, A., Radford, S. E. & Dobson, C. M. (1995). Cooperative elements in protein-folding monitored by electrospray-ionization mass-spectrometry. *J. Am. Chem. Soc.* **117**, 7548–7549.

Huang, G. S. & Oas, T. G. (1995). Submillisecond folding of monomeric lambda repressor. *Proc. Natl Acad. Sci. USA,* **92**, 6878–6882.

Ikai, A. & Tanford, C. (1971). Kinetic evidence for incorrectly folded intermediate states in the refolding of denatured proteins. *Nature,* **230**, 100–102.

Jackson, S. E. & Fersht, A. R. (1991). Folding of chymotrypsin inhibitor 2. 1. Evidence for a two-state transition. *Biochemistry,* **30**, 10428–10435.

Kern, G., Kern, D., Schmid, F. X. & Fisher, G. (1995). A kinetic-analysis of the folding of human carbonic-anhydrase-II and its catalysis by cyclophilin. *J. Biol. Chem.* **270**, 740–745.

Kiefhaber, T., Kohler, H-H. & Schmid, F. X. (1992). Kinetic coupling between protein folding and prolyl isomerization. *J. Mol. Biol.* **224**, 217–229.

Kornblihtt, A. R., Umezawa, K., Vibe-Pederson, K. & Baralle, F. E. (1985). Primary structure of human fibronectin - differential splicing may generate at least 10 polypeptides from a single gene. *EMBO J.* **4**, 1755–1759.

Kragelund, B. B., Robinson, C. V., Knudsen, J., Dobson, C. M. & Poulsen, F. M. (1995). Folding of a four-helix bundle: studies of acyl-coenzyme A binding protein. *Biochemistry,* **34**, 7217–7224.

Kragelund, B. B., Hojrup, P., Jensen, M. S., Schjerling, C. K., Juul, E., Knudsen, J. & Poulsen, F. M. (1996). Fast and one-step folding of closely and distantly related homologous proteins of a four-helix bundle family. *J. Mol. Biol.* **256**, 187–200.

Leahy, D. J., Aukhil, I. & Erickson, H. P. (1996). 2.0 Å crystal-structure of a 4-domain segment of human fibronectin encompassing the RGD loop and synergy region. *Cell,* **84**, 155–164.

Main, A. L., Harvey, T. S., Baron, M., Boyd, J. & Campbell, I. D. (1992). The 3-dimensional structure of the 10th type-III module of fibronectin - an insight into RGD-mediated interactions. *Cell,* **71**, 671–678.

Mardon, H. J. & Grant, K. E. (1994). The role of the 9th and 10th type-III domains of human fibronectin in cell-adhesion. *FEBS Letters,* **340**, 197–201.

Mines, G. A., Pascher, T., Lee, S. C., Winkler, J. A. & Gray, H. B. (1996). Cytochrome *c* folding triggered by electron transfer. *Chem.Biol.* **3**, 491–497.

Miranker, A. & Dobson, C. M. (1996). Collapse and cooperativity in protein folding. *Curr. Opin. Struct. Biol.* **6**, 31–42.

Myers, J. K., Pace, C. N. & Scholtz, J. M. (1995). Denaturant *m* values and heat capacity changes: relation to changes in accessible surface areas of protein unfolding. *Protein Sci.* **4**, 2138–2148.

Nall, B. T. & Landers, T. A. (1981). Guanidine hydrochloride induced unfolding of yeast iso-2 cytochrome *c*. *Biochemistry,* **20**, 5403–5411.

Nozaki, Y. (1972). The preparation of guanidine hydrochloride. *Methods Enzymol.* **26**, 43–51.

Onuchic, J. N., Wolynes, P. G., Luthey-Schulten, Z. & Socci, N. D. (1995). Toward an outline of the topography of a realistic protein folding funnel. *Proc. Natl Acad. Sci. USA,* **92**, 3626–3630.

Orengo, C. A., Jones, D. T. & Thornton, J. M. (1994). Protein superfamilies and domain superfolds. *Nature,* **372**, 631–634.

Pace, C. N. (1986). Determination and analysis of urea and guanidine hydrochloride denaturation curves. *Methods Enzymol.* **131**, 267–280.

Plaxco, K. W. & Dobson, C. M. (1996). Time-resolved biophysical techniques in the study of protein folding. *Curr. Opin. Struct. Biol.* **6**, 630–636.

Plaxco, K. W., Spitzfaden, C., Campbell, I. D. & Dobson, C. M. (1996). Rapid refolding of a proline rich all β-sheet fibronectin type III domain. *Proc. Natl Acad. Sci. USA,* **93**, 10703–10706.

Sali, A., Shakhnovich, E. & Karplus, M. (1994). How does a protein fold? *Nature,* **369**, 248–251.

Schindler, T., Herrier, M., Marahiel, M. A. & Schmid, F. X. (1995). Extremely rapid protein folding in the absence of intermediates. *Nature Struct. Biol.* **2**, 663–673.

Schmid, F. X. & Blaschek, H. (1981). A native-like intermediate on the ribonuclease A folding pathway. *Eur. J. Biochem.* **114**, 111–117.

Sosnick, T. R., Mayne, L., Hiller, R. & Englander, S. W. (1994). The barriers in protein folding. *Nature Struct. Biol.* **1**, 149–156.

Spitzfaden, C. S., Grant, R. P., Mardon, H. J. & Campbell, I. D. C. (1997). Module-module interactions in the cell binding region of fibronectin: stability, flexibility and specificity. *J. Mol. Biol.* **265**, 565–579.

Edited by P. E. Wright

(Received 6 February 1997; received in revised form 12 May 1997; accepted 13 May 1997)